Available online at www.sciencedirect.com
SCIENCE DIRECT®
Atmospheric Environment 40 (2006) 445–456
ATMOSPHERIC ENVIRONMENT
www.elsevier.com/locate/atmosenv

Retrieval of black carbon and specific absorption over Kanpur city, northern India during 2001–2003 using AERONET data

Sagnik Dey[a], S.N. Tripathi[a,*], Ramesh P. Singh[a], B.N. Holben[b]

[a]*Department of Civil Engineering, Indian Institute of Technology, Kanpur 208016, India*
[b]*NASA Goddard Space Flight Center, Greenbelt, MD, USA*

Received 30 April 2005; received in revised form 5 September 2005; accepted 12 September 2005

Abstract

Column-integrated aerosol black carbon (BC) concentration, [BC] has been retrieved over Kanpur (an industrial city in the Gangetic basin, northern India) during 2001–2003 for the first time. [BC] is derived from BC volume fraction and AERONET-retrieved size distribution using Maxwell–Garnett and Bruggeman mixing rules in a mixture of water, BC and $(NH_4)_2SO_4$. In addition partly absorbing components like organic carbon (OC) and dust are added to the Maxwell–Garnett mixture depending on the season to investigate their role in the retrieval of [BC]. The volume fraction of each component is retrieved by matching the mixture refractive index (real, $n(\lambda)$ and imaginary, $k(\lambda)$) with AERONET-retrieved refractive index. [BC] shows seasonal variations with high values ($>10\,mg\,m^{-2}$) observed during the post-monsoon and winter seasons and low values ($<6\,mg\,m^{-2}$) during the monsoon season. Specific absorption cross-section (α_a) decreases non-linearly with the increase in [BC], however, the decrease becomes linear when other absorbing components are present. Yearly averaged [BC] and α_a are 9.99 ± 1.95, 5.52 ± 1.07, $7.9\pm1.53\,mg\,m^{-2}$ and 7.9 ± 1.83 and 9.67 ± 3.45, $12.74\pm2.92\,m^2\,g^{-1}$ for 2001, 2002 and 2003, respectively, using Maxwell–Garnett mixing, which differ by ~15% from those using Bruggeman mixing. [BC] shows diurnal variation with morning and afternoon peaks and mid-day minimum. The amplitude is subdued as it represents the total column, which is more influenced by anthropogenic activities than by boundary layer dynamics. In order to estimate [BC] accurately, OC has to be considered when the absolute difference between $k(0.44\,\mu m)$ and $k(1.02\,\mu m)$ becomes higher than 0.0015. The sensitivity of [BC] due to dust $n(\lambda)$ becomes important during the intense dust loading period. It was found that [BC] is more sensitive to dust $k(\lambda)$ than dust $n(\lambda)$, as [BC] increases ~10–13% for 10% rise in $k(\lambda)$. Retrieved [BC] shows good agreement with the in situ measurements. Therefore our retrieval can be used as an alternate method to infer BC and OC specific absorption globally.

Keywords: Aerosols; Black carbon; Specific absorption; Internal mixing; Effective medium approximation

1. Introduction

Black carbon (BC) is the most dominant solar radiation absorbing component of aerosols causing a global mean forcing of $0.3\,W\,m^{-2}$, reducing the direct radiative effect of sulfate aerosols by 50–100% (IPCC, 2001). Several studies have confirmed that BC forcing depends on its mixing state (Fuller et al., 1999; Jacobson, 2001; Chandra et al., 2004). Specific absorption (α_a) of BC (absorption per unit mass of BC), an important optical

*Corresponding author. Fax: +91 5122597395.
E-mail address: snt@iitk.ac.in (S.N. Tripathi).

1352-2310/$ - see front matter © 2005 Elsevier Ltd. All rights reserved.
doi:10.1016/j.atmosenv.2005.09.053

parameter for characterizing BC absorption, also varies depending on the mixing state, morphology, complex refractive index and density (Fuller et al., 1999; Schuster et al., 2005). BC affects the regional hydrological cycle through evaporation of cloud droplets due to absorption of sunlight (Ramanathan et al., 2001a; Menon et al., 2002) and can be a potential health hazard (Horvath, 1993).

Sato et al. (2003) have shown that the present BC emission inventories have to be increased by a factor of 2–4 to match with the Aerosol Robotic Network (AERONET) measurements of single scattering albedo. Their results show the difficulty as well as the necessity of proper estimation of column-integrated BC concentration (in $mg\,m^{-2}$), [BC], to quantify α_a in order to assess their impact on regional climate. Studies during the Indian Ocean Experiment (INDOEX) have revealed significant amount of BC over the tropical Indian Ocean during the winter monsoon season (Ramanathan et al., 2001b; Mayol-Bracero et al., 2002; Satheesh et al., 2002). However, few measurements of surface BC concentration have been carried out in India (Babu and Moorthy, 2002; Venkataraman et al., 2002; Latha and Badarinath, 2003), which is believed to be the major source of pollution in the adjacent oceans. Recently, Tripathi et al. (2005a) have measured surface BC concentration in an industrial site in the Ganga basin (Kanpur, 80°20′E; 26°26′N, Fig. 1), northern India for 1 month (December 2004) period during Indian Space Research Organization-Geosphere Biosphere Program (ISRO-GBP) Land Campaign II. High BC concentration (6–20 $\mu g\,m^{-3}$) has been observed in the region resulting in atmospheric absorption of $\sim +71\,W\,m^{-2}$, which translates into a lower atmospheric heating rate of 1.8 K per day; three times higher than the heating rate observed over the Indian Ocean (0.5 K per day) (Satheesh et al., 2002). These results show the importance of long-term measurements of BC in the region, which is nonexistent till now. Also aerosol optical properties derived from AERONET data show high concentration of absorbing aerosols particularly during the winter season (Singh et al., 2004), which requires quantitative study to understand the radiative forcing in the region.

Recently, Schuster et al. (2005) have used Maxwell–Garnett mixing rule (MG) to retrieve [BC] globally from a mixture of BC and $(NH_4)_2SO_4$ (AS) embedded in water host. They have found that the yearly averaged α_a varies in between 7.7 and $12.5\,m^2\,g^{-1}$. In addition to MG, we have used Bruggeman effective medium approximation (Brug)

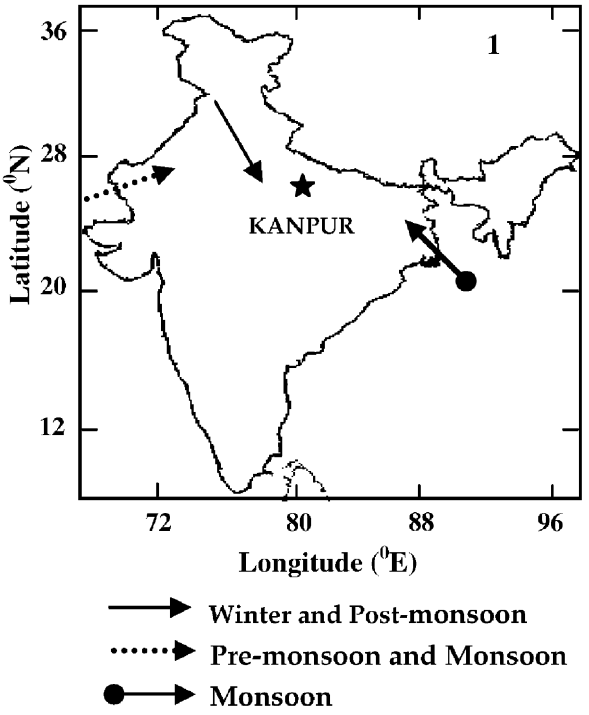

Fig. 1. Location of the study area with the regional air mass in different seasons shown by arrows.

to retrieve [BC] from AERONET data for the measured columnar volume size distribution and refractive indices. We have also considered additional partly absorbing components in our retrieval, which will be discussed in detail in the next section. The proposed retrieval technique has been validated against in-situ data from Kanpur and INDOEX. In this paper, we present, for the first time, long-term [BC] and α_a and their variability over Kanpur.

2. Retrieval of [BC] and specific absorption

We assume an internal mixture of BC, AS, water and organic carbon (OC)/dust, whose composite refractive index needs to be computed using a suitable mixing rule. The choice of the appropriate effective medium approximation is necessary to determine the optical properties of a mixture (Chylek et al., 2000, p. 276). However, the composite refractive index can be retrieved using theoretical mixing rules, the simplest being the volume-weighted average of the refractive index of individual components. The criteria for an appropriate mixing rule in such condition depend mainly on the geometric arrangement of the components constituting the mixture (Lesins et al., 2002). Two

most common mixing rules, MG and Brug, used for this study consider the dielectric constant (ε) of individual component in the calculation. As ε of different aerosol species is not enlisted in the literature, it has been derived from the corresponding refractive index.

2.1. Maxwell–Garnett and Bruggeman mixing rules

MG assumes inclusions of insoluble particles in a host solution (Fig. 2(a)) (Bohren and Huffman, 1998; Chylek et al., 2000; Lesins et al., 2002). If all the inclusions are spherical, the effective dielectric constant for the mixture (ε_{MG}) is given by (Bohren and Huffman, 1998, p. 217):

$$\varepsilon_{MG} = \varepsilon_m \left[1 + \frac{3\left(f_1 \frac{\varepsilon_1 - \varepsilon_m}{\varepsilon_1 + 2\varepsilon_m} + f_2 \frac{\varepsilon_2 - \varepsilon_m}{\varepsilon_2 + 2\varepsilon_m} + f_3 \frac{\varepsilon_3 - \varepsilon_m}{\varepsilon_3 + 2\varepsilon_m} \right)}{1 - \left(f_1 \frac{\varepsilon_1 - \varepsilon_m}{\varepsilon_1 + 2\varepsilon_m} - f_2 \frac{\varepsilon_2 - \varepsilon_m}{\varepsilon_2 + 2\varepsilon_m} - f_3 \frac{\varepsilon_3 - \varepsilon_m}{\varepsilon_3 + 2\varepsilon_m} \right)} \right]. \quad (1)$$

Here, ε_m, ε_1, ε_2 and ε_3 are the dielectric constants of the host matrix (water), BC, AS and OC/dust and f_1, f_2 and f_3 are the corresponding volume fractions of BC, AS and OC/dust, respectively.

Brug treats the components (inclusions and the host) on equal basis and is symmetric with respect to interchanging of components (Fig. 2(b)) (Chylek et al., 2000, p. 276). This is more suitable for a mixture of insoluble species where the dry aerosol species are interspersed (Lesins et al., 2002). Bruggeman effective dielectric constant (ε_B) is given by (Bohren and Huffman, 1998, p. 227):

$$\sum_{i=1}^{n} f_i \left(\frac{\varepsilon_i - \varepsilon_B}{\varepsilon_i + 2\varepsilon_B} \right) = 0, \quad (2)$$

where ε_i and f_i are the dielectric constant and the volume fraction of the ith component in a n-component mixture. In case of Brug, dry mixture of BC and AS has been considered and the retrieval results are compared with MG applied to

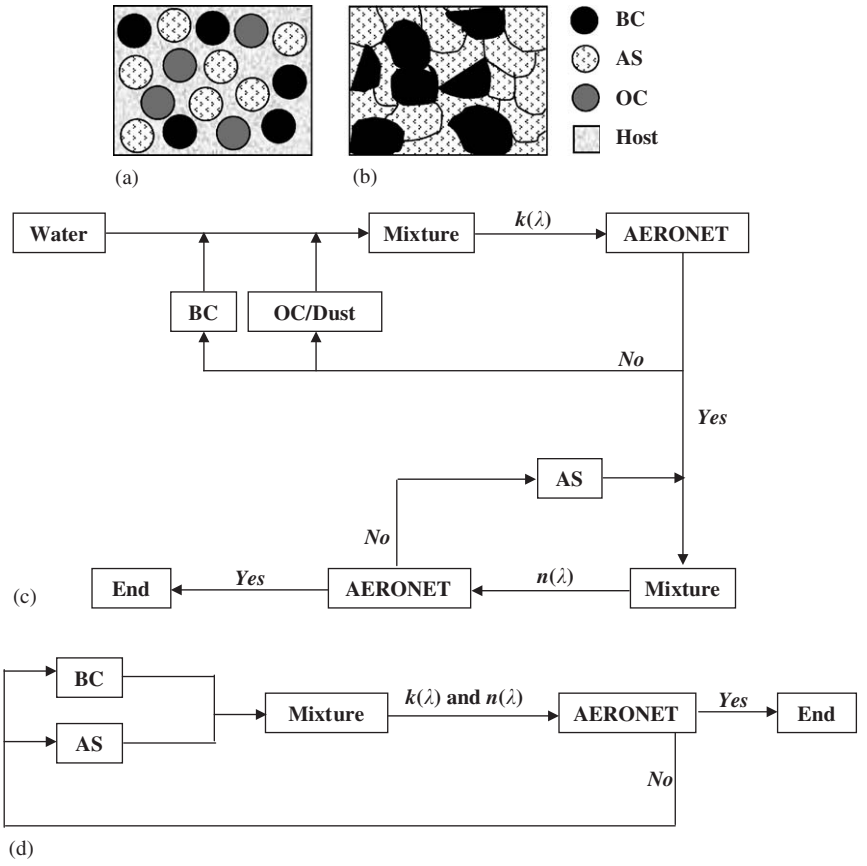

Fig. 2. Schematic representation of (a) Maxwell–Garnett and (b) Bruggeman mixing of different aerosol species and flow charts for (c) Maxwell–Garnett and (d) Bruggeman mixing rules to retrieve [BC].

three-component (BC and AS inclusions in water host) mixture for all the months.

2.2. Choice of additional partly absorbing components

OC is another light absorbing component, often coexisting with BC. OC can be differentiated from BC by its stronger spectral dependence of $k(\lambda)$ compared to BC due to enhanced light absorption at $\lambda < 0.6\,\mu m$ (Kirchstetter et al., 2004). $k(\lambda)$ retrieved by AERONET over Kanpur shows high spectral variation during the post-monsoon and winter months (October–February) (Singh et al., 2004) indicating presence of OC; hence we have considered OC as a component for these months only. During the other months, dust is considered in place of OC; because dust carried by southwesterly wind significantly affects the aerosol optical properties in the region (Dey et al., 2004) and it is also partly absorbing. The additional components like OC and dust are considered in MG mixing rule only, as it is computationally simpler than Brug mixing rule.

2.3. Application of the mixing rules for [BC] retrieval

Both MG and Brug allow the computation of the average dielectric constant of the mixture, from which the real $n(\lambda)$ and imaginary $k(\lambda)$ refractive index of mixture have been calculated using the following relations (Bohren and Huffman, 1998, p. 227):

$$k(\lambda) = \sqrt{\frac{\sqrt{\varepsilon_r^2 + \varepsilon_i^2} - \varepsilon_r}{2}} \tag{3}$$

and

$$n(\lambda) = \sqrt{\frac{\sqrt{\varepsilon_r^2 + \varepsilon_i^2} + \varepsilon_r}{2}}, \tag{4}$$

where ε_r and ε_i are the real and imaginary parts of the mixture dielectric constant.

For MG, first $k(\lambda)$ has been computed for different combinations of f_{BC} and $f_{OC/dust}$. Our interest is to determine the appropriate volume fractions of the components. f_{BC} and $f_{OC/dust}$ are adjusted until the χ^2 fit of the computed $k(\lambda)$ of the mixture is minimized with respect to the AERONET retrieved $k(\lambda)$ values by

$$\chi^2 = \sum_{i=1}^{4} \frac{(m_i^{rtrv} - m_i^{cal})^2}{m_i^{rtrv}}, \tag{5}$$

where m_i^{rtrv} is the AERONET-retrieved refractive index, m_i^{cal} is the model-calculated refractive index and i is the summation index over four retrieval wavelengths (0.44, 0.67, 0.87 and 1.02 μm) of AERONET. Once the calculated $k(\lambda)$ matches to AERONET-retrieved $k(\lambda)$ within certain range (χ^2 in the order of 10^{-3}), these volume fractions are kept constant and f_{AS} is adjusted to minimize χ^2 fit for $n(\lambda)$. As $k(\lambda)$ of AS is extremely small, it does not affect the $k(\lambda)$ of the mixture. The volume fractions of all the components for which χ^2 values of $k(\lambda)$ and for $n(\lambda)$ are lowest, are chosen as the final values to compute [BC].

In case of Brug, $k(\lambda)$ and $n(\lambda)$ are computed simultaneously. We have found that there are combinations of f_{BC} and f_{AS} for which χ^2 fit for both $k(\lambda)$ and $n(\lambda)$ have not been minimized simultaneously. For those cases, we chose the lowest χ^2 value for $k(\lambda)$ (the maximum allowable limit is 10^{-5}) to fix f_{BC}, as $k(\lambda)$ quantifies the nature of total absorption keeping in mind that χ^2 for $n(\lambda)$ would not be $> 10^{-3}$.

f_{BC} is multiplied by BC density (ρ_{BC}) and the column-integrated aerosol volume size distribution to obtain [BC] (Schuster et al., 2005):

$$[BC] = f_{BC}\rho_{BC} \int \frac{dV}{d\ln r} d\ln r, \tag{6}$$

where r is the particle radius and V is the particle volume concentration ($\mu m^3\,\mu m^{-2}$). α_a has been computed from the [BC] and the absorption optical depth (τ_a):

$$\alpha_a = \frac{\tau_a}{[BC]}. \tag{7}$$

The flow charts of the retrieval schemes using MG and Brug are shown in Figs. 2(c) and (d), respectively. BC aerosols are primarily fine mode particles; however, several studies reported their occurrences in the coarse mode, when they get attached with coarser particles (Neusüß et al., 2002; Clarke et al., 2004). Hence, they are considered to be distributed both in fine and coarse mode, as we have used the whole range of volume size distribution of AERONET retrieval ($0.005 \leqslant r \leqslant 15\,\mu m$).

For validation of our retrieval technique, we have compared our results with in-situ measurements. If one assumes BC column height to be h km, the corresponding surface BC concentration would be

$$\text{Surface BC} = [BC]/h. \tag{8}$$

2.4. Issue of refractive index

Choice of refractive index of individual component is important in our retrieval; but the refractive index of BC is not easy to measure. The detailed descriptions of the morphology and physical characteristics of different kinds of BC are given by Fuller et al. (1999). We have chosen soot G, A and B type, widely used in standard models (Fuller et al., 1999) and OPAC type, which has been used in Optical Properties of Aerosols and Clouds model by Hess et al. (1998). We have taken the average [BC] retrieved using the four above-mentioned BC types to avoid confusion about the choice of most appropriate BC refractive index, as no literature exists for this in this region. Our approach is supported by the study of Schuster et al. (2005), who have found that α_a is maximum for G-type and minimum for OPAC-type with intermediate values for A- and B-types. During the dust-loading period, the most probable source of BC in the region is vehicular emission; hence to study the sensitivity of the dust refractive index on the [BC] in our retrieval, only G-type BC has been considered. For all components except OC, we have considered spectrally independent $k(\lambda)$; values are summarized in Table 1.

We have considered spectrally dependent $k(\lambda)$ of OC (Table 1) to retrieve [BC] more accurately, otherwise χ^2 fit of $k(\lambda)$ would not be precise due to enhanced absorption by OC at $\lambda < 0.6\,\mu m$. Although, except OC, the refractive indices of all other components are spectrally flat; all four retrieval wavelengths of AERONET are considered to account the observed spectral variability in the $n(\lambda)$ and $k(\lambda)$.

Among all the components, dust is the most critical, as the contribution of dust to the absorption is still unknown (IPCC, 2001). Clarke et al. (2004) have shown that α_a of dust in the Asian outflow to be $0.009\,m^2\,g^{-1}$. In the present study, we have tested the sensitivity of [BC] to the dust $k(\lambda)$ of 0.0055 and 0.006. Average [BC] has been presented with maximum possible range of variation from mean for the dust $n(\lambda)$ in the range 1.53–1.56. The results are compared with the three-component MG mixture (no dust) during same time period.

2.5. AERONET data base

AERONET is an automated federated network of more than 200 ground-based sun/sky-scanning radiometers distributed throughout the world (Holben et al., 1998). Kanpur is one such location (Fig. 1), where the radiometer has been deployed on Indian Institute of Technology Kanpur (IITK) campus; ~17 km away from the center of the city and is operational as of January 2001. The

Table 1
Physical and optical properties of the components at 0.55 μm wavelength except OC, whose imaginary refractive index is considered to be spectrally dependent in this study

	N	K	ρ	Comments	References
Soot G	2	1	2	Paracrystalline graphite, product of diesel exhaust	Bergstrom (1972), Janzen (1979), Hess and Herd (1993)
Soot OPAC	1.75	0.44	1	Used in OPAC model	Hess et al. (1998)
Soot A	1.95	0.66	2	Similar to prolytic graphite, less absorbing than type G	Bergstrom (1972), Hess and Herd (1993)
Soot B	1.8	0.5	1.85	Low density, more similar to amorphous carbon	Twitty and Weinman, (1971), Medalia and Richards, (1983), Janzen (1980)
Water	1.33	1.96×10^{-9}	1	Host in MG mixing	Lesins et al. (2002)
$(NH_4)_2SO_4$	1.53	10^{-7}	1.76	Most ubiquitous scattering component	Seinfeld and Pandis (1998)
OC	1.53	0.063 (0.44), 0.005 (0.67), 0.001 (0.87, 1.02)	1.8	Enhanced absorption at wavelength less than 0.6 μm	Reddy and Boucher (2004), Kirchstetter et al. (2004)
Dust	1.53–1.56	0.0055, 0.006	2.6	Partly absorbing	Sokolik and Toon (1999), Tegen et al. (1996), Sokolik et al. (1993), Lesins et al. (2002), Clarke et al. (2004)

The values in the parentheses are the corresponding wavelengths in μm. Unit of density (ρ) is $g\,cm^{-3}$.

refractive index and the aerosol volume size distribution are being retrieved inverting the sky radiance measurements (Dubovik and King, 2000). We have used level 2.0 data (quality assured) of refractive indices at four retrieval wavelengths 0.44, 0.67, 0.87 and 1.02 μm to match model derived refractive indices for retrieval of [BC]. The data during June–September, 2003 are missing due to technical problems. The uncertainty is $< \pm 5\%$ for the sky radiance measurements (Dubovik et al., 2000), but the tendency of increasing errors in retrieval of optical properties with the decrease in optical depth is higher in case of refractive index than for the case of volume size distribution (Dubovik et al., 2000).

3. Results and discussion

3.1. Temporal variation of [BC] and α_a

[BC] over Kanpur shows strong seasonal as well as diurnal variations, particularly during the post-monsoon to winter seasons. Monthly averaged [BC] and α_a at 0.55 μm wavelength retrieved using MG and Brug in absence of OC and dust over Kanpur are shown in Figs. 3(a) and (b), respectively. [BC] is shown as the mean of four types of BC, whereas the vertical bars represent the possible range of variation. Maximum [BC] ($>10\,mg\,m^{-2}$) has been found to occur during the post-monsoon and winter seasons. During this time period, relatively stable atmosphere and low boundary layer lead to poor dispersion of BC. [BC] is low ($<6\,mg\,m^{-2}$) during the monsoon season (June–August), whereas [BC] varies in between, during the pre-monsoon season (March–May). High [BC] observed in some months during the pre-monsoon season is primarily due to very high volume concentration mostly in the coarse mode (>1 μm). Yearly averaged [BC] retrieved using MG ($[BC]_{MG}$)and Brug ($[BC]_{Brug}$) are 9.99 ± 1.95, 5.52 ± 1.07, $7.9\pm1.53\,mg\,m^{-2}$ and 8.55 ± 1.88, 7.16 ± 1.77, $9.38\pm2.4\,mg\,m^{-2}$ for 2001, 2002 and 2003, respectively. Temporal variation of α_a (at 0.55 μm) for MG ($\alpha_{a,MG}$) and Brug ($\alpha_{a,Brug}$) follows reverse trend (Fig. 3(b)) as that of [BC]. Yearly averaged values of $\alpha_{a,MG}$ and $\alpha_{a,Brug}$ are 7.9 ± 1.83 and 9.67 ± 3.45, 12.74 ± 2.92 and 10.38 ± 3.71, 10.36 ± 2.36 and $9.51\pm3.84\,m^2\,g^{-1}$ for 2001, 2002 and 2003, respectively. The range of values of α_a are in good agreement with the typical value of $10\,m^2\,g^{-1}$ considered by many as standard (Horvath, 1993; Liousse et al., 1993). The difference

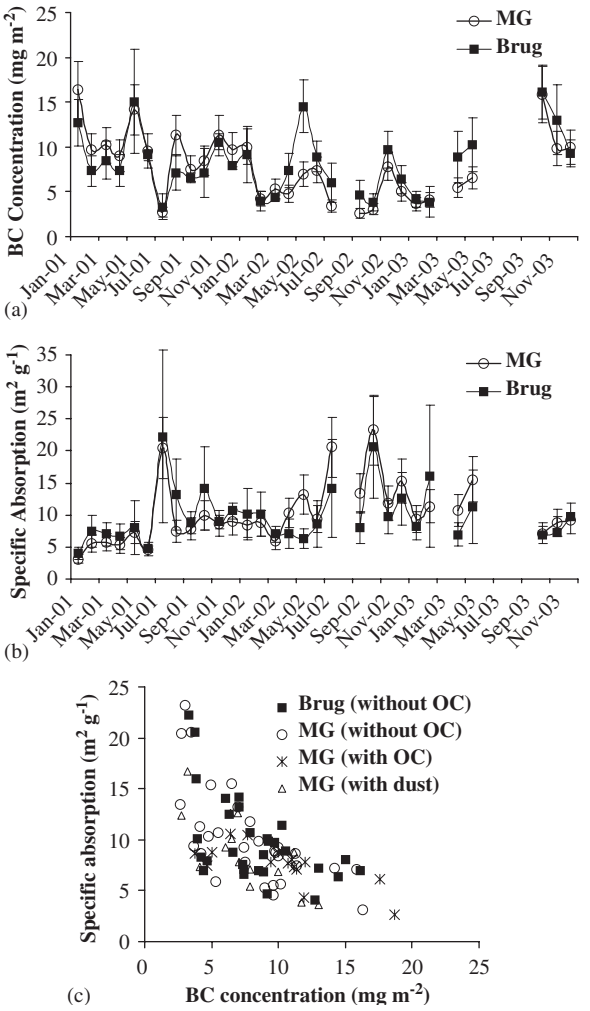

Fig. 3. (a) Monthly averaged [BC] retrieved using Maxwell–Garnett and Bruggeman mixing rules during 2001–2003. 'MG' and 'Brug' stand for Maxwell–Garnett and Bruggeman mixing rules, respectively. Each value of [BC] is averaged for four types of BC considered in this study and the vertical bars show the range of variation of [BC]. (b) Similar to Fig. 3(a), but for specific absorption cross section. (c) Scatter plot between [BC] and specific absorption cross-section for different mixing rules and combination of species.

in the yearly averaged $[BC]_{MG}$ and $[BC]_{Brug}$ is $\sim1.5\,mg\,m^{-2}$, which is ~15% of the annual average, however in few months higher discrepancy ($>3\,mg\,m^{-2}$) has also been observed. Otherwise, for most of the months, $[BC]_{MG}$ and $[BC]_{Brug}$ lie within the possible range of variation from the mean values.

$[BC]_{MG}$ and $[BC]_{Brug}$ and hence $\alpha_{a,MG}$ and $\alpha_{a,Brug}$ differ due to the difference in the mixing rules. Brug assumes randomly inhomogeneous mixture with no

specific preference of inclusions; whereas the MG distinguishes the inclusions and the embedded matrix. It is noteworthy that during the winter months when $k(\lambda)$ shows maximum spectral variation, $[BC]_{MG}$ is greater than $[BC]_{Brug}$. Fuller et al. (1999) have shown that α_a is enhanced by the increase in sulfate particle size, which in turn will reduce [BC]. Hygroscopic growth of AS is common in Kanpur during the monsoon and winter seasons, when humidity remains high (Singh et al., 2004) and it will be pronounced in case of Brug (as it is dry mixture) than MG. Hence, during the period of high relative humidity, $\alpha_{a,MG}$ is lower than $\alpha_{a,Brug}$, and subsequently $[BC]_{MG}$ is higher than $[BC]_{Brug}$.

The relationship between α_a and [BC] for different cases are shown in Fig. 3(c). In MG, BC particles are present throughout the host medium; but with the increase in f_{BC} (and hence $[BC]_{MG}$), the possibility of the presence of more BC particles in the eccentric positions increases. BC particles, at eccentric positions, are less efficient absorber (Fuller et al., 1999), hence the decrease of $\alpha_{a,MG}$ with increase in f_{BC} is not uniform. The distribution of the points in [BC]–α_a plane for Brug is similar to that for MG. Interestingly, in presence of other partly absorbing components, the relationship becomes linear, with higher rate of decrease observed in presence of dust. As, the dust particles are larger in size than OC particles, $\alpha_{a,dust}$ is greater than $\alpha_{a,OC}$. This will result in higher effective reduction of $\alpha_{a,BC}$ in presence of dust as compared to OC. Besides, OC is produced simultaneously with BC from similar source and hence the nature of internal mixing of dust and BC is different from that of BC and OC, which may play decisive role in the observed variation of $\alpha_{a,BC}$.

Diurnal variations of [BC] from 7:00 to 18:00 local time (LT) are shown in Fig. 4 as seasonal average. There is gradual increase in [BC] in the morning from 7:00 LT, reaching a maxima peak around 10:00 LT. The morning peak of BC is due to the combination of the fumigation effect in the boundary layer (Stull, 1998), where the aerosols are being brought from nocturnal residual layer after the sunrise and beginning of local anthropogenic activities. [BC] dips to a mid-day low and again shows a high peak around 14:00–15:00 LT before going down. During the pre-monsoon and monsoon seasons, afternoon peak is missing. During the daytime, increased solar heating results in increase in the boundary layer height dispersing the pollutants near the surface, whereas during the nighttime,

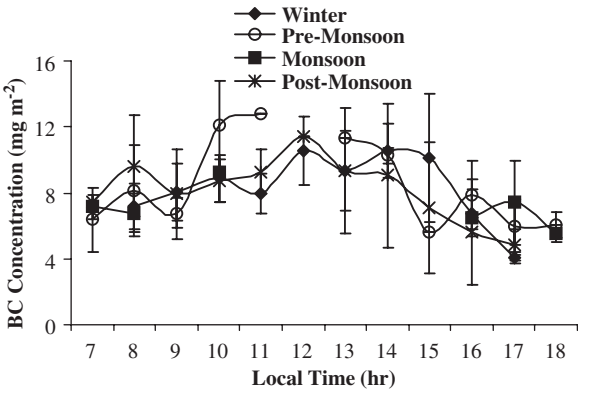

Fig. 4. Diurnal variation of [BC] (retrieved using MG mixing rule) at Kanpur seasonally averaged for 2001–2003.

the boundary layer becomes shallower resulting in entrapment of the pollutants near the surface. Until BC is removed or added in the column by some process, the diurnal variation of [BC] would not be pronounced. Hence the amplitude of the diurnal variation for the surface concentration would be higher compared to the columnar concentration, which is the case in Kanpur (Tripathi et al., 2005a) and in other continental sites (Babu and Moorthy, 2002; Latha and Badarinath, 2003). If the BC column height does not vary much diurnally, the diurnal variation of [BC] would be more controlled by the anthropogenic activities compared to the regional boundary layer dynamics. This explains the observed diurnal variation of [BC] during the pre-monsoon season. The afternoon peak, which is pronounced during the winter season, may be associated with the local anthropogenic activities under calm condition.

3.2. Role of OC in the retrieval of [BC]

Role of OC in our retrieval has been investigated, as OC is believed (as there is no in situ measurements, spectral variation of $k(\lambda)$ suggests presence of OC in significant amount, mainly during the post-monsoon and winter seasons) to affect the observed specific absorption. In Fig. 5(a), [BC] retrieved in presence of OC during October–February are plotted along with [BC] retrieved in presence of dust during March–September each year, which will be discussed in details in the next section.

An interesting finding that comes out from this study is that the [BC] in presence of OC is higher

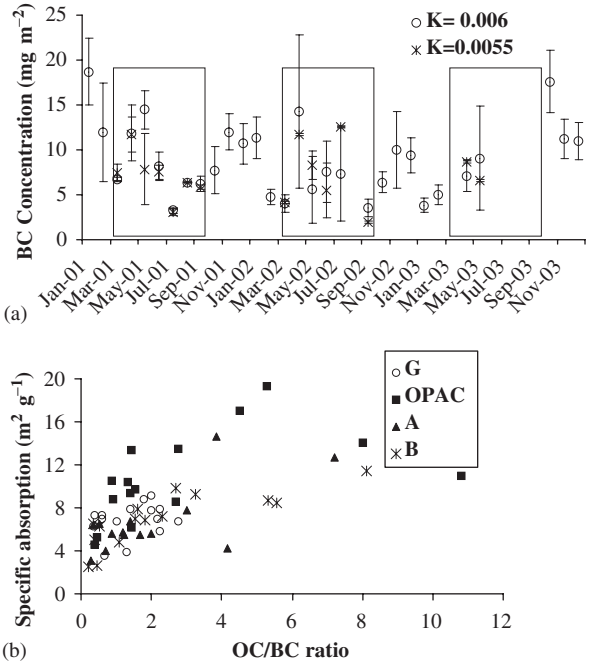

Fig. 5. (a) Monthly averaged [BC] retrieved using MG with OC as a component during October–February and dust as a component during March–September (time period shown within box). During October–February, each value represents mean of [BC] retrieved for four types of BC with the vertical bars showing the range of variation; whereas during March–September, two [BC] are shown for each month representing $k(\lambda)$ of dust 0.006 and 0.0055. Each [BC] during dust-loading period is retrieved for G-type BC and averaged for a range of $n(\lambda)$ (1.53–1.56) of dust. (b) Scatter plot between specific absorption cross section of BC and OC/BC ratio for different types of BC showing the relative contribution of OC to the absorption.

($>2\,\mathrm{mg\,m^{-2}}$) than [BC] in absence of OC (Fig. 3(a)), when the absolute difference of $k(0.44\,\mu\mathrm{m})$ and $k(1.02\,\mu\mathrm{m})$ exceeds 0.0015. In an internal mixture of AS and BC, where AS surrounds BC core, $\alpha_{a,BC}$ becomes high, as more light is focused towards absorbing BC core. When OC is present in the mixture, it may form soluble shell with AS, which causes absorption enhancement (Conant et al., 2003). In this case, some light will be absorbed by OC and hence f_{BC} should be higher to match the enhanced absorption. Our results indicate that consideration of spectral variability of OC in the retrieval is necessary for accurate estimation of f_{BC} and hence [BC], during the matching of $k(\lambda)$ with AERONET-retrieved values. Column-integrated OC concentration ([OC]) is found to vary in a wide range 2–21 $\mathrm{mg\,m^{-2}}$, with high values ($>15\,\mathrm{mg\,m^{-2}}$) being observed during November–January, when biomass burning is pronounced along with the fossil-fuel burning in Kanpur.

OC/BC ratio has been plotted against α_a in Fig. 5(b) to study the contribution of OC to the absorption. For OPAC type, α_a increases with increase in OC/BC ratio, reaching a peak at OC/BC$\sim$5.5 before going down. α_a also increases linearly with the increase in OC/BC ratio for A and B-types, but for G-type, it is almost constant. As G-type has the highest $k(\lambda)$ value, even a large increase in [OC] does not affect α_a much. The effective contribution of OC to observed α_a becomes significant after OC becomes five times higher than BC, if OPAC type BC is considered.

3.3. Effect of dust refractive index on retrieval of [BC]

Schuster et al. (2005) have avoided the dust affected sites for their retrieval due to uncertainty in the dust refractive indices, but this is necessary as dust has significant impact on the aerosol optical properties during the pre-monsoon and monsoon seasons in the Ganga basin, where large changes in single scattering albedo and $n(\lambda)$ and $k(\lambda)$ have been observed (Dey et al., 2004). The refractive index of dust is not constant, as it depends on the mineralogy of the dust particles. Several studies suggest that the real part of the dust refractive index varies in the range 1.5–1.6 (Shettle and Fenn, 1979; WMO, 1983; Sokolik et al., 1993; Tegen et al., 1996; Koepke et al., 1997; Sokolik and Toon, 1999; Dubovik et al., 2002). [BC] has been retrieved in the present study by varying $n(\lambda)$ of dust and keeping its $k(\lambda)$ constant at two representative values 0.006 (Tegen et al., 1996) and 0.0055 (Lesins et al., 2002). Soot G type has been considered in this case and each value (shown in Fig. 5(a) within box) is the average of [BC] retrieved for $n(\lambda)$ varying in the range 1.53–1.56.

We have found higher [BC] during the pre-monsoon season considering dust compared to [BC] retrieved without dust using both MG and Brug. Clarke et al. (2004) have shown that in the presence of dust, BC fraction may increase due to the uptake of BC at the surface of dust particles. The variation (reflected in the vertical bars) of [BC] due to dust $n(\lambda)$ is also high during April–June, when the region is affected by transported desert dust along with the local soil and industrial dusts. The high sensitivity may be attributed to the fluctuation in dust refractive index due to mixing

of dust arising from different sources. In 2002, the long-range transport of dust was extended beyond June (Dey et al., 2004), which is reflected in the higher variation in [BC] in July also. In general, [BC] at $k(\lambda) = 0.006$ is higher than [BC] at $k(\lambda) = 0.0055$ with a pre-monsoon maxima, the difference being greater than $3\,\mathrm{mg\,m^{-2}}$. However, in some months, the reverse trend is also observed, which is due to higher fluctuation in f_{BC} with dust $n(\lambda)$. Overall, 10% increase in dust $k(\lambda)$ results in 10–13% hike in yearly averaged [BC], which means, if more absorptive dust is present in the mixture, the variation in [BC] becomes higher. Sometimes, the variation in [BC] due to the dust refractive index is random, which may be due to the fact that dust particles are mostly non-spherical, whereas in MG, spherical inclusions are considered.

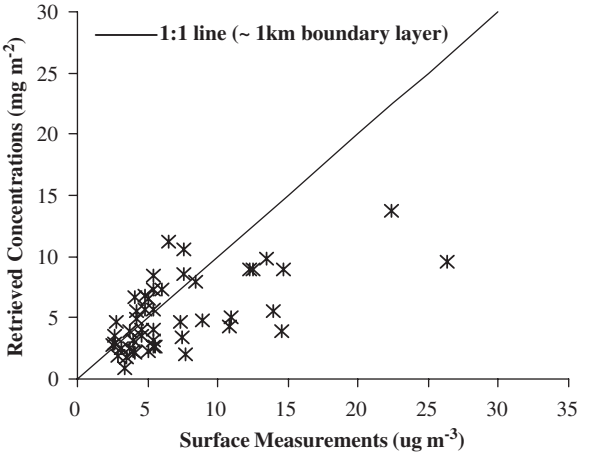

Fig. 6. Comparison between retrieved [BC] and in-situ measurements during December 2004 in Kanpur. 1:1 line represents 1 km BC column height.

3.4. Comparison with in-situ measurements

We have compared our retrieved [BC] with in situ measurements in Kanpur and INDOEX. An Aethalometer (model AE-21-ER, Magee Scientific, USA) has been deployed in IIT-Kanpur campus on December 2004 as a part of the ISRO-GBP Land Campaign-II, which enables us to compare our retrieved [BC] with the collocated surface measurements. For direct comparison, we averaged surface BC concentration measured within ± 15 min of an individual AERONET retrieval during December 2004 and compared with the corresponding [BC]. The Aethalometer was operated at 5 min time interval. The comparison is shown in Fig. 6, where the 1:1 line represents BC column height to be 1 km. There are two clusters in the scatter plot, those lying above the line represent the measurements when the BC column height is greater than 1 km and the rests represent the measurements when BC column height is less than 1 km. The average BC column height is found to be 852.6 m, which is similar to ~900 m boundary layer height measured by balloonsonde data (Tripathi et al., 2005b) during December 2004.

During INDOEX intensive field phase, BC concentration has been measured from in-situ samples collected on NCAR's C-130 aircraft in February–March 1999 (Mayol-Bracero et al., 2002). To retrieve [BC] during INDOEX period, we have chosen AERONET data of Kaashidhoo Climatological Observatory, KCO (4N, 73E) located in the islands of Maldives. Although, aircraft sampling has been done on 13 days; out of these 13 days, both level 2.0 data of refractive index and size distribution are available only for 4 days (February 18, March 7, 9, 25). As the source of the carbonaceous aerosols during INDOEX period is both fossil-fuel and biomass burning, we present [BC] as average of four BC types discussed earlier. [BC] retrieved from AERONET data during these days are 10.17 ± 2, 10.8 ± 1.9, 14.31 ± 3.7 and $14.64 \pm 2.5\,\mathrm{mg\,m^{-2}}$, respectively. The in-situ BC concentrations are reported at different altitude levels for different days, so it is not possible to calculate [BC] for direct comparison. Instead, we compared the monthly averaged values. Significant amount of OC concentration has been reported (Mayol-Bracero et al., 2002) during INDOEX period; hence [BC] has been retrieved in presence of OC using MG. The average BC concentration in the marine boundary layer (0–1.2 km) and residual continental boundary layer (1.2–3.2 km; 3.2 km is considered as the upper limit as the polluted layers are found to be present up to that height) are 2.6 ± 1 and $4.2 \pm 1.9\,\mu\mathrm{g\,C\,m^{-3}}$ in February 1999, whereas the corresponding values in March 1999 are 1.5 ± 0.7 and $2.6 \pm 1.9\,\mu\mathrm{g\,C\,m^{-3}}$, respectively (Mayol-Bracero et al., 2002). These will correspond to [BC] of 11.52 and $7\,\mathrm{mg\,m^{-2}}$, whereas [BC] retrieved from monthly averaged refractive index and size distribution data of KCO AERONET site are 11.61 ± 1.8 and $8.17 \pm 1.9\,\mathrm{mg\,m^{-2}}$. This indicates very close agreement considering the fact that [BC] is retrieved from a point source data and in-situ BC concentrations are spatially averaged.

4. Summary and conclusions

1. Schuster et al. (2005) have calculated yearly averaged [BC] in different regions of the world and they have found [BC] 0.22–0.28 $mg\,m^{-2}$ at remote islands, 0.96–3.47 $mg\,m^{-2}$ at continental sites and 2.7–3.7 $mg\,m^{-2}$ in biomass burning sites. Compared to these values, [BC] in Kanpur is much higher and it may have significant impact on the regional climate forcing. [BC] in Kanpur exhibits strong seasonal variation. Maximum [BC] ($>10\,mg\,m^{-2}$) has been found during October–January months. Yearly averaged values of $[BC]_{MG}$ and $[BC]_{Brug}$ show a difference of $\sim 1.5\,mg\,m^{-2}$, although higher difference exists in few months due to the difference in the mixing rules.
2. α_a decreases non-linearly with increase in [BC] using both MG and Brug, as increase in f_{BC} would lead to higher number of BC particles in the eccentric position of the mixture reducing the efficiency in absorption. The decrease in α_a becomes almost linear when partially absorbing OC/dust is added to the mixture. Presence of dust results in higher rate of reduction of α_a, as larger dust particles reduces $\alpha_{a,BC}$ more efficiently than smaller OC particles.
3. [BC] shows diurnal variation with morning and afternoon maximum and mid-day minimum. The morning peak is attributed to the combination of fumigation effect and commencement of anthropogenic activities. The afternoon peak, arising due to anthropogenic activities, is missing during the pre-monsoon and monsoon seasons. The amplitude of the diurnal variation is less compared to the variation of surface concentration, as it depends on the variation of BC column height controlled by seasonal meteorology.
4. Whenever, significant spectral variation of $k(\lambda)$ (i.e. $k(0.44\,\mu m) - k(1.02\,\mu m) > 0.0015$) is found, [BC] has been observed to increase in presence of OC. Therefore, in those cases, OC should be considered as a component for accurate estimation of [BC]. In Kanpur, highest [OC] ($>10\,mg\,m^{-2}$) is observed during November–January. The relative effect of OC on α_a is strongest for OPAC type and weakest for G type BC.
5. [BC] is found to be more sensitive to dust $k(\lambda)$ than to $n(\lambda)$. Only during the intense dust loading period, when dust is also transported from long range, the variation in [BC] due to dust $n(\lambda)$ becomes significant. On other hand, 10% rise in dust $k(\lambda)$ increases the yearly averaged [BC] by $\sim$10–13%, although the monthly variation is random.
6. Our retrieval technique provides an alternate, simple and independent method of retrieving [BC] in absence of in-situ measurements, as it depends on refractive index, an intrinsic property of any component. The retrieved [BC] match well with in-situ measurements. This technique can be used to study spatio-temporal distribution of BC globally, as AERONET stations are spread all over the world. However, there could be significant variation in [BC] with the dust refractive index, as mentioned in the present study. Therefore, it is required to validate the results in the sites affected by both dust and BC with in-situ measurements.

Acknowledgement

The work is supported through research project under DST-ICRP program. The CIMEL is operational on IIT Kanpur campus under AERONET program through NASA–IITK agreement. We thank the site manager and staffs for their effort in maintaining KCO site during INDOEX period. We acknowledge two anonymous reviewers for their valuable comments, which helped us improving the original version of the manuscript.

References

Babu, S.S., Moorthy, K.K., 2002. Aerosol black carbon over a tropical coastal station in India. Geophysical Research Letters 29 (23), 2098.

Bergstrom, R.W., 1972. Predictions of the spectral absorption and extinction coefficients of an urban air pollution model. Atmospheric Environment 6, 247–258.

Bohren, C.F., Huffman, D.R., 1998. Absorption and Scattering of Light by Small Particle. Wiley, New York.

Chandra, S., Satheesh, S.K., Srinivasan, J., 2004. Can the state of mixing of black carbon aerosols explain the mystery of "excess" atmospheric absorption? Geophysical Research Letters 31, L19109.

Chylek, P., et al., 2000. Effective medium approximations for homogeneous particles. In: Mischenko, M. (Ed.), Light Scattering by Nonspherical Particles: Theory, Measurements, and Geophysical Applications. Elsevier, New York, pp. 273–308.

Clarke, A.D., et al., 2004. Size distributions and mixtures of dust and black carbon aerosol in Asian outflow: physiochemistry and optical properties. Journal of Geophysical Research 109, D15S09.

Conant, W.C., et al., 2003. A model for the radiative forcing during ACE-Asia derived from CIRPAS Twin Otter and R/V *Roland H. Brown* data and comparison with observations. Journal of Geophysical Research 108 (D23), 8661.

Dey, S., Tripathi, S.N., Singh, R.P., Holben, B.N., 2004. Influence of dust storms on aerosol optical properties over the Indo-Gangetic basin. Journal of Geophysical Research 109, D20211.

Dubovik, O., King, M.D., 2000. A flexible inversion algorithm for retrieval of aerosol optical properties from sun and sky radiance measurements. Journal of Geophysical Research 105 (D16), 20,673–20,696.

Dubovik, O., Smirnov, A., Holben, B., King, M.D., Kaufman, Y.J., Eck, T.F., Slustker, I., 2000. Accuracy assessments of aerosol optical properties retrieved from Aerosol Robotic Network (AERONET) sun and sky radiance measurements. Journal of Geophysical Research 105 (D8), 9791–9806.

Dubovik, O., Holben, B., Eck, T.F., Smirnov, A., Kaufman, Y.J., King, M.D., Tanre, D., Slutsker, I., 2002. Variability of absorption and optical properties of key aerosol types observed in worldwide locations. Journal of the Atmospheric Sciences 59, 590–608.

Fuller, K.A., Malm, W.C., Kreidenweis, S.M., 1999. Effects of mixing on extinction by carbonaceous particles. Journal of Geophysical Research 104, 15,941–15,954.

Hess, M., Herd, C.R., 1993. Carbon Black. Mercel Dekker, New York.

Hess, M., Koepke, P., Schult, I., 1998. Optical properties of aerosols and clouds: the software package OPAC. Bulletin of the American Meteorological Society 79 (5), 831–844.

Holben, B.N., et al., 1998. AERONET-A federated instrument network and data archive for aerosol characterization. Remote Sensing of Environment 66, 1–16.

Horvath, H., 1993. Atmospheric light absorption—a review. Atmospheric Environment 27A (Part A), 293–317.

IPCC (Intergovernmental Panel on Climate Change), 2001. Climate change 2001: the scientific basis. In: Houghton, J.T., et al. (Eds.), Contribution of Working Group I to the Third Assessment Report of the Intergovernmental Panel on Climate Change. Cambridge University Press, New York, 881pp.

Jacobson, M.Z., 2001. Strong radiative heating due to mixing state of black carbon in atmospheric aerosols. Nature 409, 695–697.

Janzen, J., 1979. The refractive index of colloidal carbon. Journal of Colloid and Interface Science 69, 436–447.

Janzen, J., 1980. Extinction of light by highly nonspherical strongly absorbing colloidal particles: spectrophotometric determination of volume distributions for carbon blacks. Applied Optics 19, 2977–2985.

Kirchstetter, T.W., Novakov, T., Hobbs, P.V., 2004. Evidence that the spectral dependence of light absorption by aerosols is affected by organic carbon. Journal of Geophysical Research 109, D21208.

Koepke, P., Hess, M., Schult, I., Shettle, E.P., 1997. Global aerosol data set. MPI Meteorologie Humburg Rep. 243, 44pp.

Latha, K.M., Badarinath, K.V.S., 2003. Black carbon aerosols over tropical urban environment—a case study. Atmospheric Research 69, 125–133.

Lesins, G., Chylek, P., Lomann, U., 2002. A study of internal and external mixing scenarios and its effect on aerosol optical properties and direct radiative forcing. Journal of Geophysical Research 107 (D10), 4094.

Liousse, C., Cachier, H., Jennings, S.G., 1993. Optical and thermal measurements of black carbon aerosol content in different environments: variation of the specific attenuation cross section. Atmospheric Environment 27A (Part A), 1203–1211.

Mayol-Bracero, O.L., Gabriel, R., Andreae, M.O., Kirchstetter, T.W., Novakov, T., Ogren, J., Sheridan, P., Streets, D.G., 2002. Carbonaceous aerosols over the Indian Ocean during the Indian Ocean Experiment (INDOEX): chemical characterization, optical properties and probable sources. Journal of Geophysical Research 107 (D19), 8030.

Medalia, A.I., Richards, L.W., 1983. Tinting strength of black carbon. Journal of Colloid and Interface Science 40, 233–252.

Menon, S., Hansen, J., Nazarenko, L., Luo, Y., 2002. Climate effects of black carbon aerosols in China and India. Science 297, 2250–2253.

Neusüβ, C., et al., 2002. Characterization and parameterization of atmospheric particle number-, mass- and chemical size distributions in central Europe during LACE 98 and MINT. Journal of Geophysical Research 107 (D21), 8127.

Ramanathan, V., Crutzen, P.J., Kiehl, J.T., Rosenfeld, D., 2001a. Aerosols, climate and the hydrological cycle. Science 294, 2119–2124.

Ramanathan, V., et al., 2001b. The Indian Ocean experiment: an integrated analysis of the climate forcing and effects of the great Indo-Asian haze. Journal of Geophysical Research 106, 28,371–28,398.

Reddy, M.S., Boucher, O., 2004. A study of the global cycle of carbonaceous aerosols in the LMDZT general circulation model. Journal of Geophysical Research 109, D14202.

Satheesh, S.K., Ramanathan, V., Holben, B.N., Moorthy, K.K., Loeb, N.G., Maring, H., Prospero, J.M., Savoie, D., 2002. Chemical, microphysical, and radiative effects of Indian Ocean aerosols. Journal of Geophysical Research 107 (D23), 4725.

Sato, M., Hansen, J., Koch, D., Lacis, A., Ruedy, R., Dubovik, O., Holben, B., Chin, M., Novakov, T., 2003. Global atmospheric black carbon inferred from AERONET. Proceedings of the National Academy of Sciences of the United States of America 100 (11), 6319–6324.

Schuster, G.L., Dubovik, O., Holben, B.N., Clothiaux, E.E., 2005. Inferring black carbon content and specific absorption from Aerosol Robotic Network (AERONET) aerosol retrievals. Journal of Geophysical Research 110, D10S17.

Seinfeld, J.H., Pandis, S.N., 1998. Atmospheric Chemistry and Physics: From Air Pollution to Climate Change. Wiley, New York.

Shettle, E.P., Fenn, R.W., 1979. Models of aerosols lower troposphere and the effect of humidity variations on their optical properties. AFCxRL Tech. Rep. 79 0214. Air Force Cambridge Research Laboratory, Hanscom Air Force Base, MA, 100pp.

Singh, R.P., Dey, S., Tripathi, S.N., Tare, V., Holben, B.N., 2004. Variability of aerosol parameters over Kanpur, northern India. Journal of Geophysical Research 109, D23206.

Sokolik, I.N., Toon, O.B., 1999. Incorporation of mineralogical composition into models of the radiative properties of mineral aerosol from UV to IR wavelengths. Journal of Geophysical Research 104, 9423–9444.

Sokolik, I.N., Andronove, A., Johnson, T.C., 1993. Complex refractive index of atmospheric dust aerosols. Atmospheric Environment 27A, 2495–2502.

Stull, R.B., 1998. An Introduction to Boundary Layer Meteorology. Kluwer, Dordrecht.

Tegen, I., Lacis, A.A., Fung, I., 1996. The influence of mineral aerosols from disturbed soils on the global radiation budget. Nature 380, 419–422.

Tripathi, S.N., Dey, S., Tare, V., Satheesh, S.K., 2005a. Aerosol black carbon radiative forcing at an industrial city in northern India. Geophysical Research Letters 32.

Tripathi, S.N., Dey, S., Satheesh, S.K., Lal, S., Venkataramani, S., 2005b. Enhanced layer of black carbon in a north Indian industrial Indian city. Geophysical Research Letters 32.

Twitty, J.T., Weinman, J.A., 1971. Radiative properties of carbonaceous aerosols. Journal of Applied Meteorology 10, 725–731.

Venkataraman, C., Reddy, C.K., Josson, S., Reddy, M.S., 2002. Aerosol size and chemical characteristics at Mumbai, India during the INDOEX-IFP. Atmospheric Environment 36, 1979–1991.

WMO, 1983. Radiation commission of IAMAP meeting of experts on aerosols and their climatic effects. World Meteorological Organization Rep. WCP55. pp. 28–30.